Citation: Xiuxu Zhao, Yilong Lan, Jiarun Cai, et al. An experimental study on magnetic field control of polyurethane MRE seal. *Journal of Harbin Institute of Technology (New Series)*. DOI:10.11916/j.issn.1005-9113.2025108

An Experimental Study on Magnetic Field Control of Polyurethane MRE Seal

Xiuxu Zhao[1,2*], *Yilong Lan*[1,2], *Jiarun Cai*[1,2], *Yuhao Yan*[1,2] *and Haile Tang*[1,2]

(*1.School of Mechanical and Electronic Engineering, Wuhan University of Technology, Wuhan 430070, China;*
2.Hubei Key Laboratory of Digital Manufacturing, Wuhan University of Technology, Wuhan 430070, China)

Abstract: In order to meet the demand for active control of dynamic sealing contact state according to the situation in important application scenarios such as aerospace, submarine, and nuclear industry, and to achieve the goal of increasing sealing contact stress while reducing its friction and wear, this study focuses on the active control of sealing contact state of hydraulic cylinder piston rod based on polyurethane MRE, based on the adjustable and controllable mechanical properties of magnetorheological elastomer (MRE) under magnetic field. We propose a preparation scheme for prestructured polyurethane MRE sealing rings, design a magnetic control device to adjust the performance of MRE sealing rings, and study the control effect on sealing ring contact performance through control experiments. The experimental results indicate that the polyurethane MRE sealing ring is sensitive to magnetic fields, and its contact stress and friction can be significantly adjusted. This study provides a basis for further realizing intelligent adjustment and control of hydraulic reciprocating seals in practical work processes.

Keywords: polyurethane; magnetorheological elastomers; sealing contact stress; friction force; magnetic field control
CLC number: TB42;TB381;TH136 **Document code**: A **Article ID**: 1005-9113(2026)00-0000-15

0 Introduction

The polyurethane is polymerized from isocyanate and polyol compounds. Its matrix contains strong polar carbamate groups and its insolubility in nonpolar solvents gives it excellent characteristics: high mechanical strength, strong wear resistance, good water resistance, a wide hardness adjustment range, and high resilience[1-3]. This has led to its widespread use in reciprocating hydraulic cylinder seals[4-5]. The polyurethane sealing element not only can effectively prevent the hydraulic oil from mutually channeling in the chamber or leaking out of the environment through the piston rod, but it also ensures that the system will not lose its function because of leakage and cause accidents, and can effectively prevent external impurities and pollutants from invading the hydraulic system. This prevents damage to other hydraulic components, thus extending the hydraulic system's service life. For reciprocating seals, however, leakage depends not only on the choice of material but also on the seal contact status[6-7]. For the reciprocating seal, if the system needs to achieve a reliable sealing state, first, it is necessary to ensure that the sealing contact pressure is greater than the sealed oil pressure. Second, the "internal pumping effect" needs to be greater than or equal to the "external pumping effect" to ensure zero leakage[8].

The contact stress and friction force of reciprocating sealing rings are caused by changes in mechanical properties due to the contact of the sealing rings. Maintaining good contact stress is an important prerequisite for the reliable operation of reciprocating sealing systems. At the same time, in order to maintain a longer service life of the sealing system, it is necessary to reduce sealing friction during reciprocating operations. The maintenance of this sealing state traditionally depends on the mechanical properties of the seal ring itself. But as time of use increases, the seal ring begins to show irreversible changes such as wear, aging, and relaxation[9]. The

Received 2025-08-28.
Sponsored by National Natural Science Foundation of China (Grant No. 52375202).
* Corresponding author. Xiuxu Zhao, Ph.D, Professor. Email: zhaoxiuxu@whut.edu.cn.

contact stress of the seal pair drops like a cliff[10], unless the machine is shut down for maintenance. Otherwise, the system will fall into a vicious circle of uncontrolled medium leakage.

In current research, methods for compensating the mechanical properties of seal contact mainly include three aspects: optimal design of seal structures, research and development of seal materials, and monitoring of seal status. Details are as follows:

1) The optimal design of seal structures mainly focuses on developing structures such as elastic combined seals or compensating seal structures. For example, Xiao et al.[11] proposed a pressure-compensated piston scheme for concrete delivery cylinders. This scheme uses constant hydraulic pressure to maintain the pressure between the piston seal and the delivery cylinder. By maintaining the pressure between the piston seal of the concrete cylinder and the cylinder body with constant hydraulic pressure, it can solve a series of problems of the piston, including excessive initial interference, high resistance, large heat generation, high energy consumption, severe wear, and a short service life[11]. Pu et al.[12] proposed a main shaft sealing device for hydropower plants, which can realize automatic wear compensation and has a long service life cycle . Wang[13] designed a system device capable of online adjustment of compensation pressure and a multi-sensor test scheme for monitoring the seal contact status. This design can provide optimal compensation pressure values for seals with different degrees of wear. Based on the tribological mechanism of contact-type reciprocating seals, Ye et al.[14] optimized the design of plunger packing seals. They achieved this by optimally matching parameters such as plunger diameter, stroke, and pump speed, reasonably controlling the linear velocity of the plunger, and reducing friction speed. Additionally, by reasonably controlling the pressure of the flushing fluid, they ensured good lubrication of the seal pair, thereby increasing the service life of the plunger packing seal from the original 1500 h to more than 4500 h[15].

Although the optimal design of the seal structure can compensate for seal failure to a certain extent, it is difficult to control the compensation magnitude. Excessive compensation often occurs, which easily leads to the frictional heat accumulation effect[16].

2) The Research and Development (R&D) of sealing materials mainly focuses on developing sealing materials with high wear resistance. For instance, to enhance the tribological properties of PTFE (polytetrafluoroethylene) spring-actuated seals, Zhao et al.[16] modified PTFE by adding various fillers. The comparative results of tribological experiments showed that, compared with spring-actuated seals made of pure PTFE, the friction torque of those made of GF/PTFE (glass fiber-reinforced PTFE) was reduced by 28.97%. Li[17] utilized the low friction coefficient characteristic of UHMWPE (ultra-high molecular weight polyethylene) to modify MPU (milled polyurethane elastomer) to reduce friction. Tests on tribological and mechanical properties indicated that the dynamic friction coefficient of MPU/modified UHMWPE could be decreased by 33%, the wear rate by 76%, and the tensile strength increased by 9%.

Although the R&D of new sealing materials can effectively reduce the friction coefficient of seals and make up for the poor wear resistance of traditional sealing materials, they still pose risks caused by uncontrollable sudden seal failure, as they cannot directly compensate for the sealing contact stress.

3) Development of magnetically controlled intelligent sealing systems with regulatory functionality. For instance, Huanggang Normal University[18] proposed a hydraulic cylinder with internal leakage suppression based on Magnetically controlled Shape Memory Alloys (MSMAs). This design leverages the magnetically induced deformation principle of MSMAs to compensate for the defect of large leakage caused by clearance sealing[18]. However, in experiments, a strong magnetic field of over 8 Tesla (T) is required to achieve a displacement at the 1.5 μm level—an extremely high magnetic field that is difficult to provide with practical engineering devices. Meanwhile, shape memory alloys also suffer from issues such as insufficient phase transition sensitivity, phase transition broadening, and randomness in their structure, which limit their application in actual engineering scenarios.

Currently, technologies that alter the contact properties of sealing surfaces through external excitation mainly include electric fields[19], magnetic fields[20], and thermal fields[21]. Among these, electric field control requires high voltage and poses safety risks, while temperature control demands a relatively long response time. By comparison, the

magnetic field control method can balance safety and rapid response, making it a highly promising regulation approach. In relevant applications, magnetorheological fluid sealing is a non-contact dynamic sealing technology that uses magnetic liquids. It achieves an inhomogeneous magnetic field distribution by adopting a magnetic-concentrating structure that confines the magnetic liquid within the sealing gap. This forms an "O"-shaped liquid ring that fills the sealing gap to achieve sealing, and it has been widely used in gas-sealing applications[22]. However, when magnetorheological fluid sealing is applied to liquid sealing, it has limitations such as a narrow pressure resistance range and an inability to achieve long-term zero leakage[23].

Magnetorheological Elastomer (MRE) is a material where magnetic particles are dispersed in soft elastic bodies like rubber, endowing it with mechanical responsiveness to magnetic fields. Under the influence of an external magnetic field, the dynamic mechanical properties of MREs can undergo reversible changes within milliseconds[24]. Its unique rheological characteristics enable real-time regulation of mechanical properties under an applied magnetic field[25]. The unique rheological properties of MREs enable real-time regulation of their mechanical properties under the influence of an external magnetic field.

Among MRE materials, those based on polyurethane as the matrix are particularly typical. Their modulus[26] can be rapidly adjusted with the magnetic field, facilitating precise control of sealing contact stress. Due to the anisotropic mechanical properties of MREs[27], MREs can be pre-structured as needed to achieve the desired regulatory effect under the action of a magnetic field. The greater the magnetic field intensity, the higher the hardness (or compressive modulus) of MRE. After hardness enhancement, the material surface is less prone to stick-slip phenomena during sliding. The suppression of stick-slip directly leads to a reduction in the friction coefficient and wear rate. Experimental studies have shown that at low speeds, magnetic fields significantly reduce the amplitude of stick-slip, thereby minimizing wear[28].

These tunable properties enable polyurethane-based MREs to offer potential for balancing leakage and wear, promising innovative solutions for the field of hydraulic reciprocating seals. Therefore, to meet the demand for compensating for the performance of hydraulic reciprocating seals in critical applications such as aviation, submarines, and the nuclear industry, this study explores and verifies a hydraulic reciprocating seal contact mechanical property regulation and compensation scheme. This scheme not only achieves the regulation of seal contact stress but also reduces friction and wear in reciprocating seals. Section 1 introduces the preparation of polyurethane MRE seal rings, Sections 2 and 3 present the mechanical property regulation tests and result analysis of polyurethane MRE seal rings, and finally, the conclusions of this study are given.

1 Preparation of Polyurethane MRE Seal Ring

The study of polyurethane elastomers began in 1937 in Germany. They were first synthesized by Otto Bayer and his team[29] at I. G. Farbenindustrie AG through the addition polymerization of liquid isocyanates with polyethers or diol polyesters. So far, polyurethane, as a kind of synthetic polymer material, has been widely used in various fields. To obtain magnetorheological polyurethane sealing materials with relatively stable comprehensive performance, this study refers to the existing formulas of polyurethane seals for hydraulic cylinders and adopts the prepolymer method to prepare magnetorheological elastomer samples. The specific details are introduced as follows:

1) Matrix material. The prepolymer selected is a cast polyurethane elastomer with the components of polyether PTMG (polytetramethylene ether glycol) and MDI (methylene diphenyl diisocyanate). Products made with this system have the advantages of high resilience, excellent tensile and tear resistance, and good wear resistance. Its main parameters are shown in Table 1.

Table 1 Main performance parameters and sources of polyurethane prepolymer

-NCO content(%)	Hardness(A)	Viscosity (at 80 ℃)(mPa·s)	Recommended casting temperature(℃)	Supplier
5	50	800±200	110-120	Mingli Plasticization Co.

2) Chain extender. Alcohol-based chain extenders have relatively high melting points and tend to crystallize during chain extension process, which leads to internal defects in the material. In contrast, amine-based chain extenders can introduce rigid benzene rings into the material, significantly improving the mechanical properties of the final product—such as high strength and high tear strength—while providing excellent wear resistance and precise hardness control. Additionally, MOCA (3, 3′-dichloro-4, 4′-diaminodiphenylmethane) can endow the material with better heat resistance and chemical stability, enabling it to perform well in harsh environments. Its good processing adaptability also makes the casting molding process smoother, facilitating the production of high-quality polyurethane products. Therefore, solid MOCA was selected as the chain extender, and its specific parameters and appearance are shown in Table 2.

The dosage of MOCA can be calculated based on the isocyanate content in the purchased polyurethane prepolymer, with the formula as follows:

$$w_{\text{moca}} = 0.9W \cdot f \cdot n_{\text{moca}} \cdot n_{\text{NCO}} \quad (1)$$

where w_{moca} represents the calculated dosage of MOCA; W denotes the amount of polyurethane; f stands for the isocyanate content; n is the relative molecular mass of the substance, and the subscript indicates the corresponding substance.

3) Magnetic particles. The functional response of MREs is directly related to the electromagnetic properties of the internal magnetic particles. Carbonyl Iron Powder (CIP) magnetic particles exhibit soft magnetic properties—including high magnetic permeability and low coercivity—along with a smooth spherical physical morphology. They demonstrate excellent anti-agglomeration characteristics and matrix compatibility, enabling uniform dispersion in the polymer matrix, and possess rapid magnetization-demagnetization switching capability under an external field. Thus, they have become the preferred filler for preparing high-performance MREs. Therefore, this study uses micron-sized high-purity CIP as the magnetic particles for MRE preparation, and the selected magnetic particles are spherical CIP. Their specific parameters and appearance are shown in Table 3.

4) Additives. During the synthesis of MREs, magnetic particles are difficult to uniformly disperse in the matrix material, and "agglomeration" often occurs. Therefore, it is necessary to pretreat the carbonyl iron powder. The silane coupling agent KH550, used as a surfactant for the surface modification of carbonyl iron powder, can assist the fusion of carbonyl iron powder particles with the matrix material. Thus, before synthesizing polyurethane MRE materials, KH550 is first used to pretreat the surface of carbonyl iron powder at a dosage of 2 wt% relative to the iron powder content. Its specific parameters and appearance are shown in Table 4.

The preparation process flow for polyurethane MRE materials is shown in Fig. 1.

To ensure the quality and stability of the prepared materials, the following process links need to be focused on controlling:

1) Carbonyl iron powder pretreatment process.

Table 2 Main performance parameters and sources of MOCA

Chemical formula	Molecular weight	Melting point(℃)	Purity(%)	Supplier
$C_{13}H_{12}Cl_2N_2$	267.154	102-107	≥99.5	Mingli Plasticization Co.

Table 3 Parameters of carbonyl iron powder

Chemical formula	Tap density (g/cm^3)	Particle size (μm)	Purity(%)	Supplier
Fe	3.31-3.35	5,10,20	≥99.9	Guangzhou Metal Metallurgy Group

Table 4 Parameters of coupling agent

Chemical formula	Molecular weight	Weight density(g/cm^3)	Purity(%)	Supplier
$C_9H_{23}NO_3Si$	221.37	0.942	≥96.0	AVIC New Materials Technology

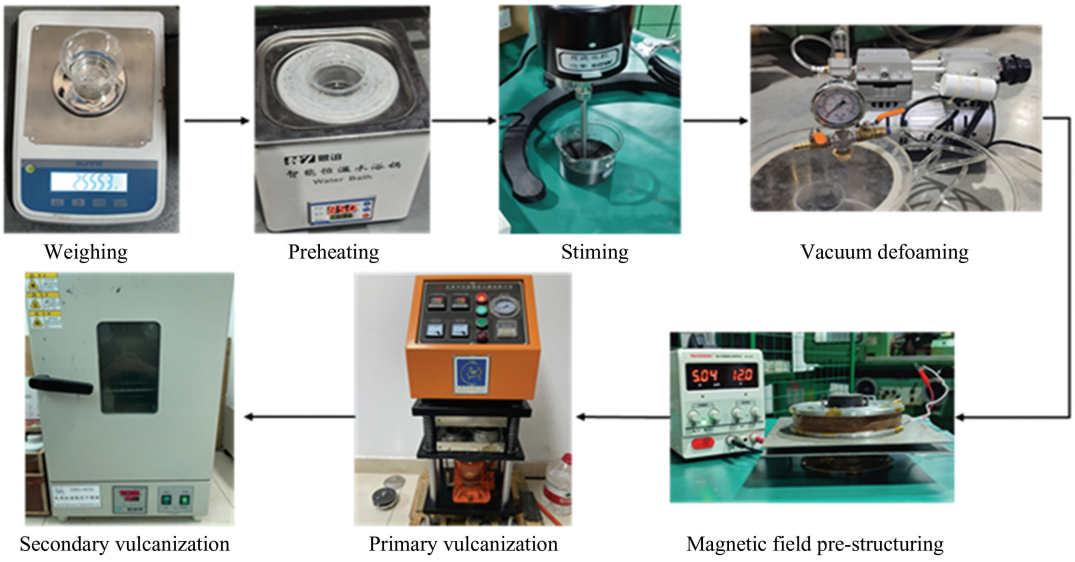

Fig.1 Preparation process of polyurethane MRE

Pretreatment: Prepare a solution by mixing the silane coupling agent with anhydrous ethanol in a certain ratio. After blending with carbonyl iron powder, adopt a combination of mechanical stirring and ultrasonic dispersion to achieve uniform coating of the coupling agent on the surface of the iron powder.

Post-treatment: Separate the solid and liquid phases of the modified suspension by vacuum filtration, then dry to remove residual solvents. Finally, break agglomerated particles via mechanical grinding to obtain surface-modified iron powder raw materials.

2) MRE casting molding process.

Mixing: Place the polyurethane prepolymer in a constant temperature environment for preheating to reduce the system viscosity and improve subsequent mixing uniformity. Keep the prepolymer sealed during preheating. Adopt a staged feeding method to add modified iron powder into the prepolymer, and achieve uniform dispersion of particles through mechanical stirring.

Defoaming: Perform cyclic degassing of the mixed system under negative pressure, controlling the defoaming time until the gas microbubbles enclosed in the mixture are effectively eliminated. Pay attention to isolating water vapor during the process.

Magnetic field-assisted curing: Apply an axial magnetic field (0 - 1T) during the material cross-linking reaction stage to promote the ordered arrangement of magnetic particles along the magnetic field lines. Pay attention to the curing time to prevent iron powder sedimentation and aggregation.

The purpose of this study is to explore the regulation experience of MRE sealing rings. Therefore, rectangular MRE sealing rings with a relatively simple structure were prepared to complete the sealing state regulation test. By referring to the radial seal groove dimension table in the national standard GB/T 3452.3-2005[30], it is found that when the piston rod diameter is 50 mm and the seal groove depth is 5 mm, the recommended cross-sectional diameter of O-rings or rectangular rings is 6.0307 mm. Checking the hydraulic piston rod dynamic seal groove dimension table in the same standard, the inner diameter of the O-ring or rectangular ring is 51.5 mm, and the outer diameter is 63.5614 mm (rounded to 63.6 mm). At this time, the compression rate of the sealing ring is 17.36%, which exactly falls within the recommended compression rate range of 0% - 20.0% for the corresponding cross-sectional diameter, meeting the requirements. Based on this, the mold for preparing polyurethane MRE sealing rings is designed as shown in Fig.2.

To ensure the reliability of the experimental results, the prepared samples need to be surface-treated before the sealing performance test. The treatment is divided into two operations: firstly, a scraper is used for removing the macroscopic burrs from the sealing ring loop; secondly, high-mesh sandpaper is used to gently polish and clean the surface with absolute ethanol.

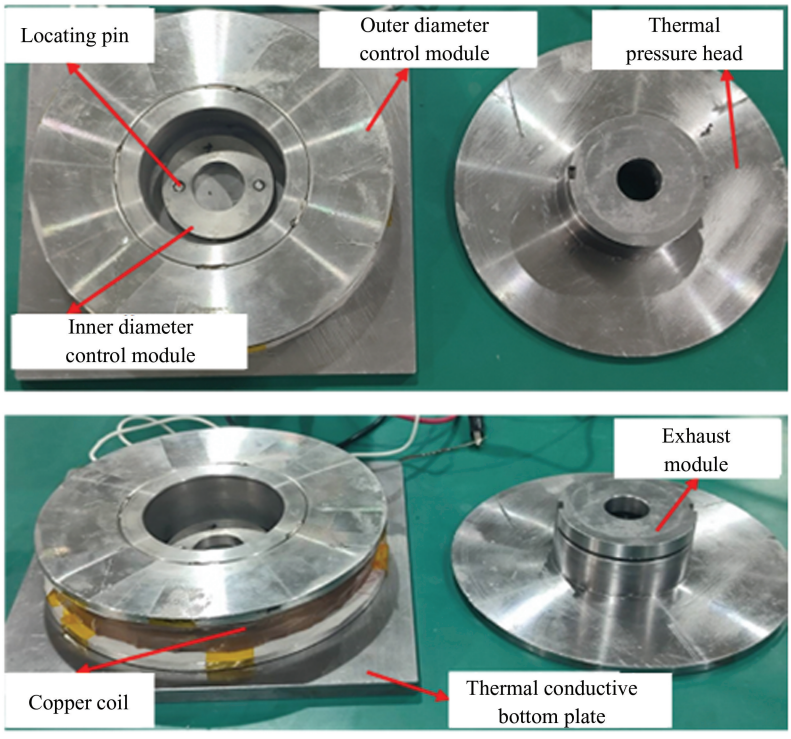

Fig.2 Preparation of the mold of MRE seal ring

2 Sealing Contact Mechanical Property Regulation and Control Test Scheme

2.1 Test Device

As shown in Fig.3, a test cylinder was designed according to the national standards GB/T 15622-2023[24] and GB/T 15242.3-2021[25] to test whether the MRE sealing ring achieved adjustable contact stress and friction force. The experimental hydraulic cylinder is installed on the electronic universal material testing machine; its accuracy class is 0.5 (±0.5 % of full scale (FS)), as shown in Fig.3(a). The internal structure of the test cylinder is shown in Fig.3 (b). The blue marked position in Fig.3 (b) is the groove of the normal sealing ring, and the red marked position is the sealing groove of the MRE sealing ring. The MRE sealing ring shown in Fig.3 (c) is installed in it. There is no piston in the test cylinder, and its up and down reciprocating motion is driven by the motor of the universal testing machine.

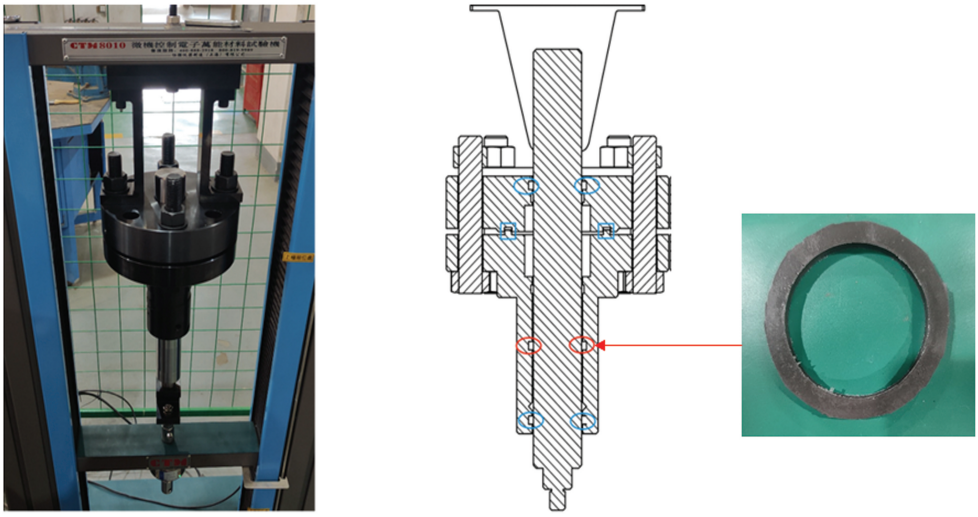

(a) Test cylinder (b) The internal structure of test cylinder (c)MRE seal ring

Fig.3 MRE sealing ring and test device

2.2 Monitoring Program

Seal friction and contact stress can reflect the working state of the seal ring, so for a specific monitoring and regulation scheme, it is necessary to monitor and control contact stress and friction.

To clarify the transformation process and interrelationship between the outer wall deformation of the hydraulic cylinder and the contact strain and stress of the internal sealing ring, a simulation verification of the transmission of the sealing contact pressure was first conducted. A simulation model was established for the test device used in the experiment, with a test temperature of 25 ℃, a rod speed of 10 mm/s, a friction coefficient of 0.1, and a wall thickness of 10 mm. Simulation analyses were performed on the reciprocating stroke of the hydraulic rod at no oil pressure and 20 MPa oil pressure, respectively, to verify the transmission law of the contact pressure on the sealing surface of the sealing ring to the outer surface of the test cylinder under the experimental conditions.

As shown in Fig. 4, the model used for simulation is a two-dimensional axisymmetric model, which mainly comprises three parts: the test cylinder barrel, the MRE sealing ring (with a Poisson's ratio of 0.45 and an elastic modulus of 23.0725 MPa), and the hydraulic rod (with a Poisson's ratio of 0.3 and an elastic modulus of 209 GPa). For the rod seal, the contact surface between the sealing ring and the hydraulic rod serves as the primary sealing surface, while the remaining contact surfaces are secondary sealing surfaces. The primary sealing surface is surface M_1, the secondary sealing surface is surface M_2, and the outer wall of the test device corresponding to the secondary sealing surface is surface M_{2f}. To balance computational accuracy and efficiency, the optimal parameters were determined through grid convergence verification: the initial grid size was set to 0.5 mm and gradually refined to 0.1 mm, with additional refinement applied to the grids of the key monitoring models M_2 and M_{2f}. The final model has a total of 13425 elements and 41530 nodes. Verified using the ANSYS Grid Quality Check tool, the average aspect ratio is 1.0404, and the average overall grid quality is 0.9926, which meets the accuracy requirements for 2D axisymmetric structural analysis.

Boundary condition settings:1) Fixed constraint: A fixed constraint was added to the upper wall of the cylinder block based on the characteristics of actual assembly, to simulate the fixed state of the structure after actual installation; 2) Displacement load: "Displacement" was applied, causing the piston rod to generate a displacement of 0.28 mm along the *Y*-direction while remaining free in other directions; 3) Contact setting: The model involves 2D contact between multiple components. Frictional contact was adopted for the contact interface, with a friction coefficient set to 0.1, ensuring that the force and displacement transmission in the contact area conform to real-world conditions.

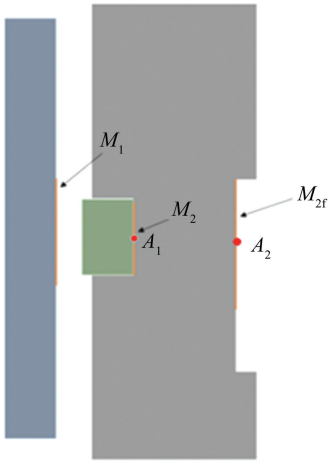

(a) The main surface(s) in the simulation model

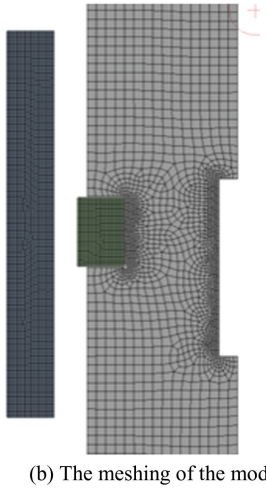

(b) The meshing of the model

Fig. 4 Surface and mesh generation in the simulation model

Under preload compression, both the primary and secondary sealing surfaces of the MRE sealing ring can achieve full contact with the hydraulic rod, providing initial contact pressure.

As shown in Fig.5, it is the Von Mises stress distribution of the MRE sealing ring under precompression, and the stress distribution is mainly

affected by the cross-sectional shape of the seal, the size of the seal groove, and the compression ratio. With its structural characteristic of a rectangular cross-section, the rectangular MRE sealing ring can achieve full contact between its upper and lower sealing surfaces with the primary and secondary sealing surfaces under preload compression.

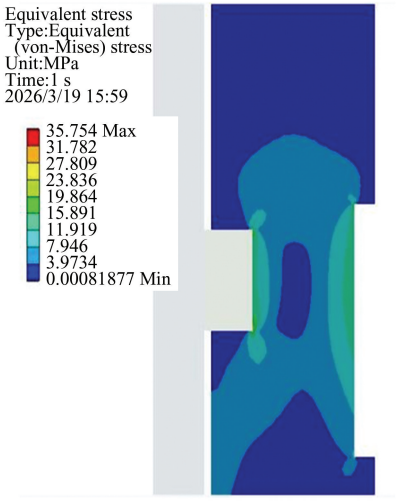

Fig.5 Von Mises stress distribution contour diagram of the secondary sealing surface to the outer surface of the test device

Fig.6 shows the normal elastic strain distribution from the secondary sealing surface to the outer surface of the test device. Its stress distribution is mainly affected by cross-sectional dimensions, groove structure, and compression ratio, with stress areas concentrated primarily at the edges and end faces where the sealing ring contacts the primary and secondary sealing surfaces.

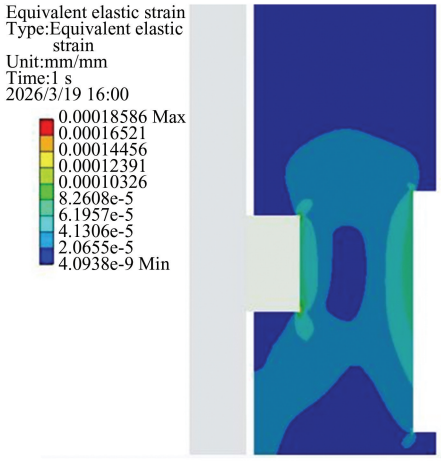

Fig.6 Contour diagram of normal elastic strain distribution from the secondary sealing surface to the outer surface of the test device

Through elastic deformation induced by preload compression, the rectangular sealing ring generates uniform, stable contact pressure on both the primary and secondary sealing surfaces, providing a reliable guarantee of initial sealing.

In the simulation results, the strains on the sealing surface M_2 and the outer surface M_{2f} of the test device were extracted separately, and the results are shown in Fig. 7.

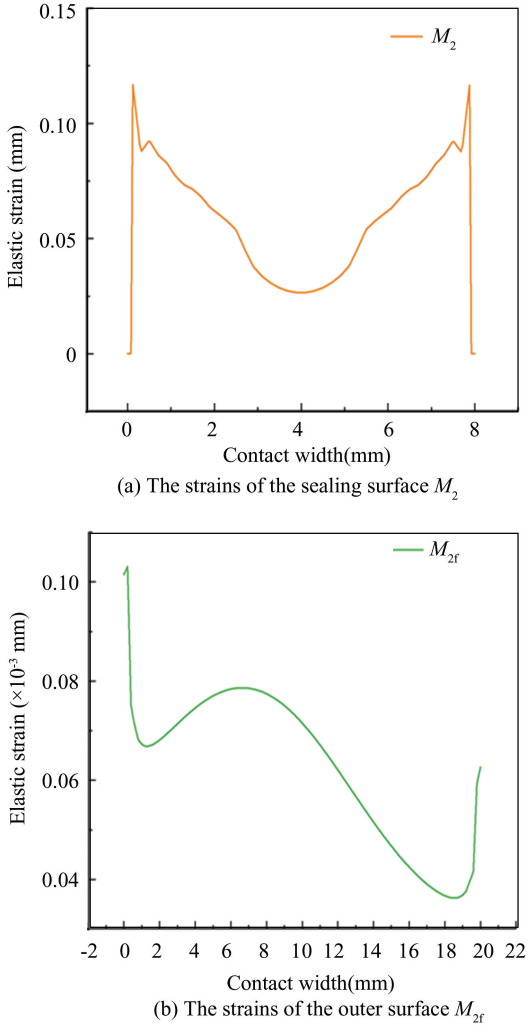

Fig.7 The strains of the sealing surface and the outer surface

As shown in Fig. 7(a), the maximum strain in the rectangular-section MRE sealing ring acting on the secondary sealing surface M_2 is concentrated at the two edges. After the strain is transmitted to the outer surface M_{2f} in Fig. 7(b), the shape of the strain distribution curve changes, and the position of the maximum strain shifts by 2−3 mm along the extrusion direction of the rectangular-section MRE sealing ring. The peak point of strain corresponds exactly to the

relative position between the MRE sealing ring and the outer surface M_{2f} of the test device (as shown in Fig. 4). Based on the above analysis, this study attaches fiber Bragg grating sensor closely to the outer wall of the hydraulic cylinder to sense the deformation of the hydraulic cylinder cylinder caused by the compression of the sealing ring. The sensor system is composed of SMF-28 single-mode optical fiber, with its grating region having an effective length of 10 mm. The initial spectral characteristics show a wavelength range of 1510–1590 nm and a reflection efficiency exceeding 90%. The strain sensing unit is arranged on the outer surface of the cylinder at the position corresponding to the seal groove structure, and the dynamic sensing of contact stress is realized by analyzing the wavelength shift of the grating.

The working pressure range of the test cylinder is 0–25 MPa, the safety check pressure is 37.5 MPa, the inner diameter of the cylinder is 52 mm, and the material of the cylinder is 45 steel. The allowable stress is taken as 140 MPa, and the safe wall thickness of the material is calculated to be 7 mm. The strength and safety inspection of the thinning results for the outer wall of the hydraulic cylinder was conducted through finite element simulation, to increase deformation at the sensor position on the outer wall of the hydraulic cylinder while ensuring strength. The maximum value increased from 0.69 μm to 0.88 μm, an increase of 27.5%.

To obtain the deformation at M_2 through the sensor, it is necessary to establish the strain relationship between M_2 and M_{2f}. Extract the deformation of M_2 and M_{2f} at the middle point of the seal ring when the seal ring is compressed by 10% – 20%, and the gradient is 2%, these refer to points A_1 and A_2 in Fig. 4 (a). The deformation at the corresponding position is linearly fitted, as shown in Fig.8, where R refers to the correlation coefficient of the fitting result.

Therefore, after the sensor is used to monitor the outer wall of the hydraulic cylinder, the deformation of the cylinder wall at the sealing contact area can be calculated using the formula. And then the contact stress level of the secondary sealing surface sealing pair is calculated.

To monitor the friction force, a microcomputer-controlled electronic universal material testing machine with its force sensor is used. The model is HBM-U10M/10kN from Germany, which is used to measure the change in the system test force indication before and after excitation to determine whether MRE can reduce the seal friction.

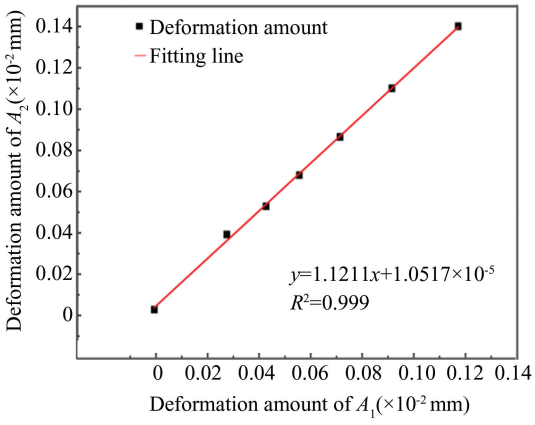

Fig.8 Corresponding relationship of deformation amount in *Y* direction between M_2 and M_{2f}

2.3 Regulation and Control Scheme

The magnetic fluid elastomer sealing ring regulating and controlling device is fixed on the outer side of the lower cylinder head of the original hydraulic cylinder 3. The structure is shown in Fig.9.

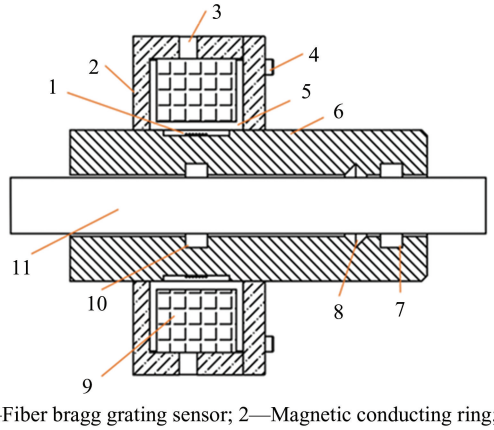

1—Fiber bragg grating sensor; 2—Magnetic conducting ring; 3—Lead groove; 4—Bolt; 5—Coil holder; 6—Cylinder outer wall; 7—Normal sealing ring sealing groove; 8—Oil collection tank; 9—Electromagnetic coil; 10—MRE sealing groove; 11—Piston rod

Fig.9 Sealing control scheme

The electromagnetic coil 9 is supported by the testing coil framework 5 and can generate a corresponding magnetic field intensity at the sealing groove 10 according to different currents. This thereby changes the elastic modulus of the MRE and realizes the active regulation and control of the contact stress on the sealing surface of the piston rod. Besides, that experimental scheme also considers the condition that the magnetorheological elastomer seal ring cannot seal the leakage. The oil collecting groove 8 is used for

collecting leakage caused by poor sealing of the magnetorheological elastomer sealing ring. The normal seal ring is installed in the seal groove 7 to prevent oil leakage that could pollute the environment.

Establish a 1 ∶ 1 two-dimensional symmetrical control unit model in ANSYS' Maxwell module for magnetic circuit simulation analysis, as shown in Fig.10.

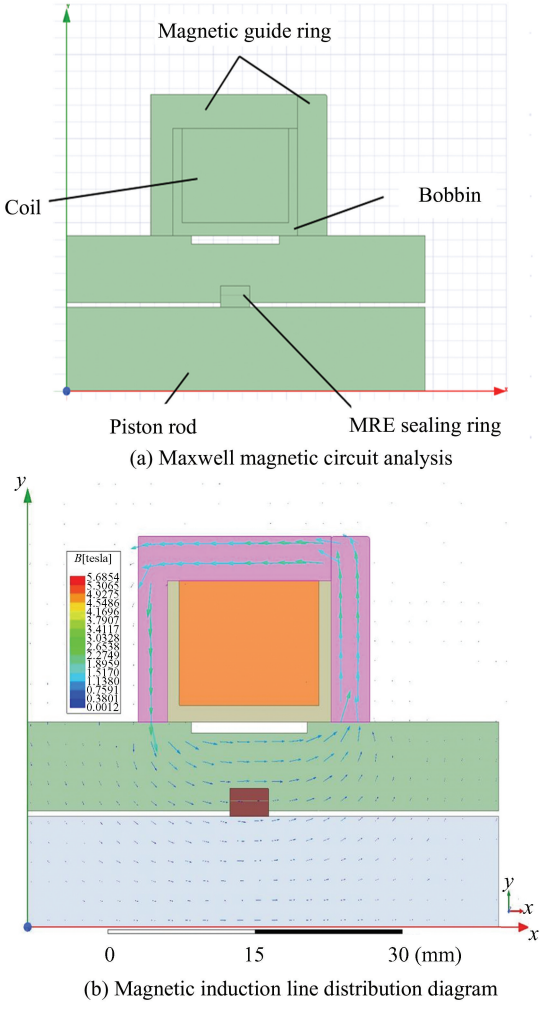

Fig.10 Magnetic field simulation of the magnetization device

To evaluate the magne tic field excitation effect of the MRE seal ring, a reference line was established along the thickness direction in the central area of its cross-section. The magnetic flux density data were obtained by sampling the magnetic induction intensity on the baseline in Maxwell software. Through the statistical analysis of discrete points, the average characteristics and gradient variation law of the overall magnetic induction intensity of the seal ring can be characterized. Set the excitation range to 500 – 3500 ampere-turns and the gradient to 1000 ampere-turns. As a result, as shown in Fig.11, it can be seen that the magnetic field intensity at the two ends of the selected straight line (i.e., at the edge of the seal ring) is significantly higher than that in the middle region (B is the magnetization in mT). The difference is about 155 mT, which is caused by the larger permeability of the cylinder barrel than MRE.

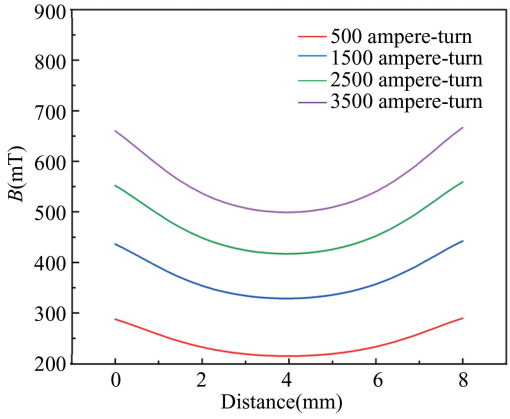

Fig.11 Distribution of magnetic field intensity on the centerline of MRE seal ring

As shown in Fig.11, the ordinate B represents the magnetic field strength, and simulation results indicate that when the excitation generated by the excitation coil exceeds 2500 ampere-turns, the magnetic flux density exerted on the MRE reaches over 400 mT, which is close to the saturation magnetic field requirement of the prepared polyurethane-based MRE. Therefore, based on the laboratory power supply's maximum output current of 5 A and the minimum excitation requirement of 2500 ampere-turns, the wire quantity required for winding is calculated, and the number of turns of the excitation coil is approximately 500 – 700 turns. Considering that more turns lead to higher resistance and more heat generation at the same current, this study selects 600 turns as the final number of turns for the external electromagnetic coil. The dimensions of the excitation coil framework are 85 mm × 134 mm × 34 mm, the wire diameter is 0.8 mm, the winding length is about 211 m, and the maximum excitation capacity is 3000 ampere-turns. The average value of the data is taken as the average magnetic field strength of the MRE sealing ring, and the fitted relationship between the theoretical magnetic flux density of the magnetic field generating device and the current is shown in Fig.12.

Fitting the current of the DC power supply and the magnetic flux density of the MRE to obtain a functional relation between the magnetization and the

excitation current:

$$B = 63.68I + 198.85 \quad (2)$$

where I is the excitation current in A.

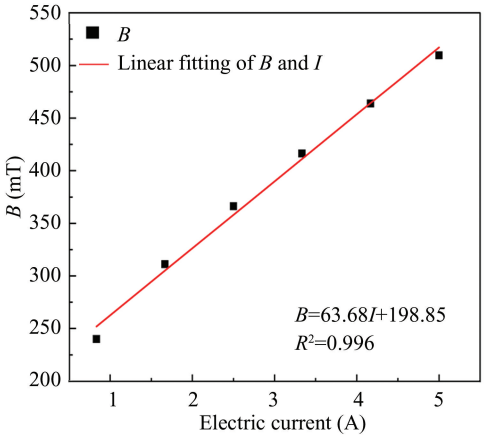

Fig.12 Fitting curve of magnetic field and current

3 Analysis of Regulation Test Results

To verify whether polyurethane MRE has adjustable, controllable effects on hydraulic cylinder testing, and magnetic mechanical performance tests were conducted. The on-site experimental setup is shown in Fig.13. The MRE seal ring is installed in the sealing groove of the test hydraulic cylinder (marked by the red circle in the figure), and the installation position of the magnetic control device corresponds to the sealing groove.

The MRE sealing magnetic field control verification test is divided into two parts: 1) Change the current, set the range of the electrifying current of the exciting coil to be 0−4 A, the gradient to be 1 A, the piston rod does a up-and-down reciprocating motion, the maximum reciprocating stroke is 100 mm, and the speed is 15 mm/s. Observe and record the change of the system resistance to explore the friction performance of the magnetic control MRE seal ring; 2) The piston rod was still, and the current was changed every 30 s, with the change value of 1 A each time, and the change of the wavelength of the fiber grating was observed and recorded. To explore the magnetic control contact stress change effect of the MRE seal in the hydraulic cylinder.

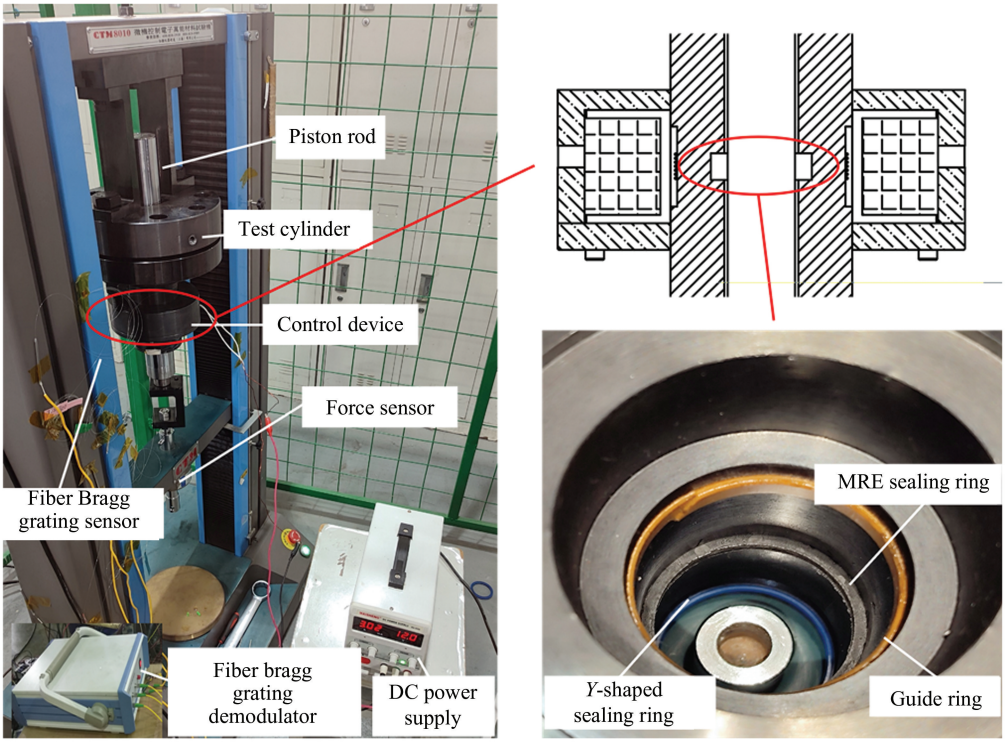

Fig.13 Magnetic field control test of MRE seal ring

Because the test time is short and the heat of the electromagnetic coil is small, the influence of temperature on the wavelength offset of the FBG is not considered. Without considering temperature change and wave guide effect (influence of fiber grating axial deformation on refractive index)[30], the relationship between the wavelength shift and the strain is obtained.

$$\lambda_B = (1 - p_e)\lambda_B \Delta\varepsilon = K_\varepsilon \Delta\varepsilon \quad (3)$$

where K_ε is the strain sensitivity of FBG sensors, and P_e is approximately 0.22 at room temperature[31]. From Eq.(3), it can be seen that the offset of the FBG center wavelength $\Delta\lambda_B$ is positively correlated with the FBG strain. Because the FBG strain $\Delta\varepsilon$ is caused by the deformation of the outer wall of the hydraulic cylinder, the greater the deformation of the outer wall, the greater the $\Delta\varepsilon$. In addition, the hydraulic cylinder is made of metal material, and according to Hooke's law, the stress of the metal material is proportional to the strain when it is in the elastic deformation stage. Stress is proportional to strain. Therefore, it can be concluded that when the magnetic field is applied to the magnetorheological elastomer seal ring to change its mechanical properties, if the characteristic wavelength shift amount $\Delta\lambda_B$ is positive, the seal contact stress will increase. The characteristic wavelengths obtained from testing with MRE seal rings and without MRE seal rings are shown in Fig.14.

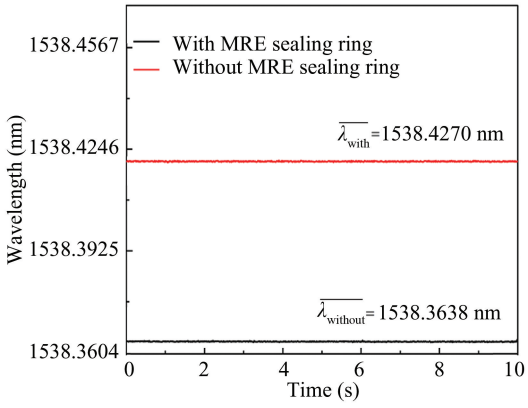

Fig.14 Comparison of time-domain signals of FBG sensors before and after installing MRE seal

Before installing the sealing ring, the average characteristic wavelength of the FBG sensors was 1538.3638 nm, which is the initial characteristic wavelength of FBG sensors. After the installation of the MRE seal ring, the contact stress generated on the main sealing surface and auxiliary sealing surface due to the compressive force between the piston rod and the sealing ring will cause deformation of the inner and outer walls of the hydraulic cylinder, resulting in an increase in the characteristic wavelength of the fiber Bragg grating. According to Eq. (3), the wavelength drift of the FBG sensors can be calculated to be 56.9 pm. To calculate the contact stress of the sealing surface, it is assumed that the FBG sensors are completely attached to the outer wall of the hydraulic cylinder. The axial strain of the FBG sensors is equal to the radial strain of the outer wall attachment surface, the radial strain of the outer wall is:

$$\varepsilon_j = \nu_g \Delta\varepsilon_h \quad (4)$$

where v_g is the Poisson's ratio of the hydraulic cylinder, with a value of 0.3. Therefore, the radial strain of the outer wall of the hydraulic cylinder is 1.4220×10^{-5}, and the deformation is 0.1423 μm. According to the formula fitted in Fig. 11, the deformation at the corresponding position on sealing surface A_2 is 0.1790 μm. Since the elastic modulus E of 45 steel is 209 GPa[32], the deformation is in the elastic range. The contact stress of the sealing pair can be calculated by the formula $P = \varepsilon_j \times E$ and the calculation result is 3.9478 MPa.

Since the test system includes multiple sealing components (e.g., guide bands and regular sealing rings), it is difficult to directly measure the friction force of the MRE sealing ring. Therefore, this study uses changes in the overall system resistance as a substitute for the friction force. The specific operation steps are as follows: 1) Complete the extension and retraction strokes of the piston rod without installing the sealing ring, and acquire the corresponding tension and pressure values during this process via the testing machine sensor; 2) Complete the extension and retraction strokes of the piston rod with the MRE sealing ring installed, and obtain the tension and pressure values during this process through the testing machine sensor; 3) Calculate the difference between the tension and pressure values in the two scenarios, which is the change in the overall system resistance.

It is difficult to directly measure the friction value of the MRE seal ring because the system contains many seals, such as the guide belt and *Y* shaped sealing ring. A change in that magnitude of the overall resistance of the system is therefore contemplated instead of a frictional force. When other conditions are kept unchanged, only the magnitude of the electrified current in the excitation coil is changed, and the system resistance is reduced. It shows that the friction of the sealing pair becomes smaller and has the effect of magnetic control friction reduction, which is conducive to prolonging the sealing life. The test results are shown in Fig.15.

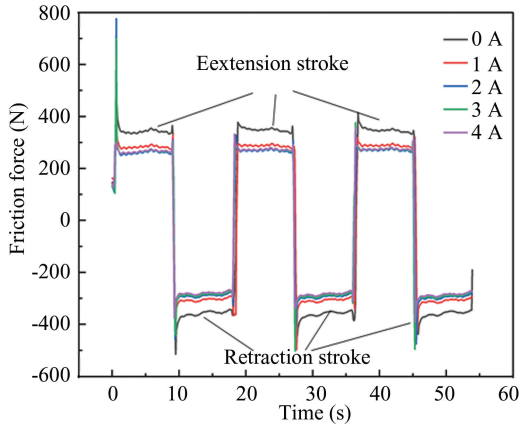

Fig. 15 Friction force variation under different current excitations

Taking the upward movement of the piston rod as the extension stroke, it can be seen from Fig.15 that there is a peak point of test force when the piston rod is just started or changes direction, which is caused by the transition of friction from static friction to dynamic friction. When there is no magnetic field and the current is 0 A, the friction force of the stable stage system is about 358 N. When the current of the electromagnetic coil is changed, the system resistance decreases regardless of the extension or retraction stroke. When the current is 1 A, the friction force is about 305 N, which decreases by about 14.8%. As the current increases, the friction force of the system further decreases, then gradually tends to stabilize. This is because when the current reaches 4 A, the simulated magnetic field is about 450 mT, approaching the material's saturation magnetic field strength. At this time, the system friction force is about 278 N, with a decrease of 22.3%.

As shown in Fig. 16, when the piston rod is stationary and the current is changed every 30 s, the characteristic wavelength of the FBG sensor gradually increases with the current. After 150 s, the power is cut off instantly, and the characteristic wavelength immediately returns to its initial level. This indicates that the MRE seal ring has a significant control effect and a more sensitive response in the hydraulic cylinder. From the data collected at each magnetic field strength, extract the difference between the characteristic wavelength of the Fiber Bragg Grating (FBG) sensor at the end of each segment and the initial wavelength, and use this difference as the characteristic wavelength variation. Then, calculate the variation of the magnetic contact stress of the MRE seal after energization based on this wavelength variation. The average contact stress results obtained at each magnetic field strength are shown in Table 5.

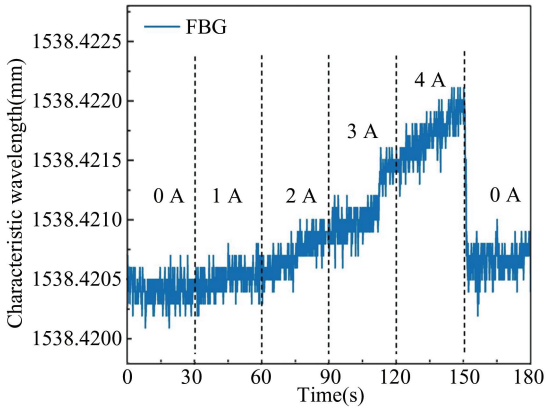

Fig.16 Change of FBG characteristic wavelength under different current

Table 5 Change of seal contact stress under different current

Current size (A)	Magnetic flux density (mT)	Average contact stress (MPa)	Rate of change (%)
0	0	3.9478	—
1	262.53	3.9545	0.1697
2	326.21	3.9674	0.4964
3	389.89	4.0065	1.4869
4	453.57	4.0390	2.3102

The test results show that the control device designed in this paper is effective, and that the external magnetic field can indeed alter the contact stress on the sealing surface. With the increase of the magnetic flux density, the contact stress of the sealing pair gradually increases, and its rate of change increases with the increase of the magnetic flux density. At the theoretically simulated magnetic flux density of 453.57 mT. The change rate of contact stress is about 2.3102%.

4 Conclusions

This study is based on the magnetic control characteristics of MRE and has completed the following work:

1) A hydraulic dynamic seal active control scheme was proposed, which integrates fiber optic grating sensors to monitor the sealing contact stress in real time, tension and pressure sensors to read the sealing friction force in real time, and uses electromagnetic coils to dynamically adjust the MRE

elastic modulus and friction coefficient to compensate for the sealing interface pressure and reduce the sealing friction force. A "state sensing parameter analysis magnetic field control" sealing contact mechanical performance feedback mechanism was established.

2) Designed and optimized a hydraulic cylinder testing bench, and verified through simulation and safety verification that thinning the cylinder wall to 9 mm can increase the deformation of the outer wall by 27.5% and significantly improve sensor sensitivity.

3) Developing an external magnetic circuit control device, combined with Maxwell simulation and experimental verification, confirmed that when the excitation current reaches 4 A, the sealing contact stress can be increased by 2.31%, and the frictional force can be reduced by 22.3% synchronously.

4) The sealing ring control test shows that the polyurethane MRE seal ring prepared in this study exhibits a sensitive magnetic response and significant adjustability of contact stress and friction performance, providing theoretical and technical support for the intelligent control of hydraulic dynamic seals.

Existing research has shown that temperature can affect the softness and hardness of the matrix and the magnetization of magnetic particles, thereby affecting the magnetorheological effect of MRE. At present, performance comparison experiments at different temperatures have not been conducted during testing. Therefore, in future research, we plan to use temperature as a parameter variable to reveal the temperature sensitive response mechanism of MRE seal rings in hydraulic reciprocating sealing systems, providing theoretical support for optimizing magnetic control sealing performance under extreme temperature conditions.

Statements and Declarations

• Availability of data and materials: Data is available upon request from the authors.

• Conflicts of Interest Declarations: All authors declare that they have no conflicts of interest.

References

[1] Li Y, Zhou M, Wang R, et al. Self-healing polyurethane elastomers: An essential review and prospects for future research . European Polymer Journal, 2024, 214: 113159. DOI: 10.1016/j.eurpolymj.2024.113159.

[2] Zhang T, Huo S, Ye G, et al. Tough, high-strength, flame-retardant and recyclable polyurethane elastomers based on dynamic borate acid esters . Reactive and Functional Polymers, 2024, 205: 106056. DOI: 10. 1016/j. reactfunctpolym.2024.106056.

[3] He Q P, Xu J. Development and engineering application of main drive super-large PU sealing ring of shield machine. China Rubber Industry, 2022, 69(12): 932-938.

[4] Yang J, Li Y H, Chen S B, et al. Study on poly (urethane-urea) elastomers as sealing material fortunneling boring machine's main drive . Acta Polymerica Sinica, 2023, 54 (12): 1857 - 1869. DOI: 10. 11777/j. issn1000 - 3304.2023.23159.

[5] Li C. Analysis on leakage problem of hydraulic support column in coal mining work face. Mechanical Management and Development, 2021, 36(3): 281-282.

[6] Nikas G K. Performance mapping of rectangular-rounded hydraulic reciprocating seals to minimize leakage, frictional work and abrasive wear with the aid of a duty parameter. Tribology International, 2023, 179: 108191. DOI: 10.1016/j.triboint.2022.108191.

[7] He J S, Guo F, Wu F, et al. Research on the Influence of Size Deviation on Sealing Performance Based on ABAQUS Simulation. Lubrication Engineering, 2022, 47(6): 37-44.

[8] Muller H. Fluid Sealing Technology: Principles and Applications. New York: Routledge, 2019.

[9] Liu X, Yang J, Wang M, et al. Life Prediction of rubber O-shaped sealing ring with accelerated aging method. China Rubber Industry, 2025, 72(1): 66-69.

[10] Chen C, Wu G, Fu X L, et al. Design optimization of thermal shock-resistance double - cone seal structure of pressurizer. Nuclear Power Engineering, 2018, 39 (4): 176-181. DOI: 10.13832/j.jnpe.2018.04.0176.

[11] Xiao X L, FU J Q. Study on the sealing structure of piston for the concrete conveying cylinder with the type of pressure compensation. Construction Machinery, 2016(4): 61-63.

[12] Pu H J, Xiao Y, Ding H Q, et al. Application and research of wear compensation type main shaft seal for bulb tubular units. China Plant Engineering, 2021(23): 93-94.

[13] Wang R. Design and Experimental Study of Pressure Compensated Hydraulic Reciprocating Seal. Wuhan: Wuhan University of Technology, 2019.

[14] Ye X Y, Ding Y N, Xu J Q, et al. Research on improvement of reciprocating seal life of special piston pump. Drainage and Irrigation Machinery, 2009, 27(6): 373-378.

[15] Peng C, Yu H, Qi S B, et al. Research on seawater hydraulic reciprocating seal characteristics under bilateral high-pressure. Chinese Hydraulics & Pneumatics, 2025, 49(1): 40-49.

[16] Zhao X, Li S, Liu D, et al. Material optimization method for a spring-energized seal based on wear analysis. Lubricants, 2024, 12 (8): 288. DOI: 10. 3390/

lubricants12080288.
[17] Li J. Antifriction Modification and Application Research of Polyurethane Sealing Washer. Wuhan: Hubei University of Technology, 2015.
[18] Huanggang Normal University. A hydraulic cylinder with internal leakage suppression based on magnetic control shape memory alloy. China: 201910532045.6. 2024-09-13.
[19] Tsala S, Berthier Y, Mollon G, et al. Numerical analysis of the contact pressure in a quasi-static elastomeric reciprocating sealing system. Journal of Tribology, 2018, 140(6): 064502. DOI: 10.1115/1.4040154.
[20] Barron E J III, Williams E T, Tutika R, et al. A unified understanding of magnetorheological elastomers for rapid and extreme stiffness tuning. RSC Applied Polymers, 2023, 1(2): 315-324. DOI: 10.1039/D3LP00109A.
[21] Xu Y, Gong X, Xuan S, et al. A high-performance magnetorheological material: preparation, characterization and magnetic-mechanic coupling properties. Soft Matter, 2011, 7(11): 5246-5254. DOI: 10.1039/C1SM05301A.
[22] Kiarie W M, Gandha K, Jiles D C. Temperature-dependent magnetic properties of magnetorheological elastomers . IEEE Transactions on Magnetics, 2021, 58(2): 1-5. DOI: 10.1109/TMAG.2021.3082302.
[23] Wang J. Preparation and Performance Experimental Study of Polyurethane-based Magnetorheological Elastic Polishing Pad. Xiangtan: Xiangtan University, 2021.
[24] National Technical Committee 3 on Hydropneumatic of Standardization Administration of China. Hydraulic Fluid Power: Sealing Devices. Standard Test Methods to Assess the Performance of Seals Used in Oil Hydraulic Reciprocating Applications: GB/T 32217-2015. Beijing: Standards Press of China, 2015.
[25] National Technical Committee 3 on Hydropneumatic of Standardization Administration of China. Hydraulic Cylinder—Test method: GB/T 15622 - 2023. Beijing: Standards Press of China, 2023.
[26] National Technical Committee 3 on Hydropneumatic of Standardization Administration of China. Dimensions Series of Rod and Piston Dynamic Seals for Hydraulic Cylinders—Part 3: Dimensions And Tolerances of Groove for Co-Axial Seals: GB/T 15242. 3 - 2021. Beijing: Standards Press of China, 2021.
[27] Cheng H, Chen X, Chen X, et al. Research on key factors of sealing performance of combined sealing ring . Applied Sciences, 2022, 12(2): 714. DOI: 10.3390/app12020714.
[28] Bai S, Wang T, Yang J. An experiment on the dwell time effect of rubber seal o-rings: friction force in intermittent reciprocating motion. Materials, 2024, 17(10): 2427. DOI: 10.3390/ma17102427.
[29] Bayer O, Siefken W, Rinke H, et al. Verfahren zur Herstellung von Polyurethanen und Polyharnstoffen. Germany: DRP 728981. 1937-11-13.
[30] National Technical Committee 3 on Hydropneumatic of Standardization Administration of China. Housing dimensions for O-ring elastomer seals in hydraulic and pneumatic applications: GB/T 3452. 3 - 2005. Beijing: Standards Press of China, 2005.
[31] He C J, Li P, He C F, et al. High-sensitive magnetic field sensor based on Terfenol-D and fiber bragg grating. Journal of Mechanical Engineering, 2025, 61(8): 1-8. DOI: 10.3901/JME.2025.08.001
[32] Dong Y F, He K, Yu W, et al. Study on stress test and influence factors of connecting bolt of automobile hub bearing. Bearing, 2025, 3: 1-9.